

Study on the Fluid-Solid Interaction Mechanism of Caohe Aqueduct in South-to-North Water Diversion Middle Line Project Under Condition of Seismic Loads

PENG Hui¹ LIU De-fu² TIAN Bin³

¹Dr. College of Civil & Hydroelectric Engineering of China Three Gorges University, Yichang,, China

²Professor, College of Civil & Hydroelectric Engineering of China Three Gorges University, Yichang,, China

³Professor, College of Civil & Hydroelectric Engineering of China Three Gorges University, Yichang,, China

E-mail:hpeng1976@163.com

ABSTRACT: Based on considering the fluid-solid coupling problem in aqueduct, the dynamic FEM model of fluid-solid interaction was established by use of Galerkin Method. And the seismic response of Caohe aqueduct structure in the South-to-North Water Diversion Middle Line Project was calculated. The results indicate that seismic response of the aqueduct structure increases with the rise of water level, and so the fluid-solid interaction was of great influences on the seismic response of the aqueduct structure. The calculated results could provide good instruction to forthcoming aqueduct construction and operational management and safety monitoring.

KEYWORDS: aqueduct; fluid-solid interaction; seismic response; dynamic characteristics; South-to-North Water Diversion Project

1.INTRODUCTION

In engineering community, the fluid-solid interaction between some structures in fluids and fluids itself is a common problem that we often encounter. There is an extensive meaning for projects construction to study the problem of fluid-solid interaction. The problem of fluid-solid interaction was firstly put forward by H. M. Westergaard in the 1930s[1]. In China, Prof. Zheng Zhe-min took some researches on coupled vibration between water and plates and cantilever in 1950s[2~3]. In the period of 1960s to 1970s, the study on fluid-solid interaction in overseas was active and the main research objects concentrated on hydraulic structures and different ships which occurred coupled vibration caused by water waves. The theory of hydroelasticity was established by a British specialist R. E. D.Bishop at that time[5~7]. At present, generally there are two methods which can be used to research the problem of fluid-solid interaction. The first one is analytical-numerical simulation, Geers double asymptotic approximation(DAA) commonly used so far[8]; the second one is numerical method, including FEM, BEM, Lagrange-Eulerian Method and so on. In linear fluid-solid interaction system(linear elastic structures and ideal incompressible fluid), there are also two methods often used to study fluid-solid interaction problem. The first one is through taking displacement vectors of structures and fluids as field variables to research fluid-solid interaction problem, such as displacement-displacement scheme[9~10]; the second one is to use hybrid scheme which comes from structures displacement vector and fluid field variables, such displacement-pressure scheme, displacement-velocity potential scheme and so on[11~12]. In FEM, if the fluids are incompressible the method of Numerical Computing Method of Additional Water Mass is often applied [13~14].

When we consider the character of fluids compressibility, the Galerkin Method is applied to construct fluid-solid interaction FEM formulas between aqueduct and water in this paper. The research indicates that numerical method can simulate the coupling interaction between water and huge water-retaining structures and seismic response well.

2.CALCULATION PRINCIPLE

Fluid-solid interaction problem is very complicated and it involves in structure dynamics and fluids dynamics. Usually, some supposes can be made according to practical engineering problems. As a result, the calculation model will be simplified and efficiency will be improved effectively. In this paper, we not only consider big structures coupled vibration, but also consider the interaction between water and big structures under condition of small fluctuation. In practical calculation, in order to make calculation convenient we often suppose that fluids are inviscid and irrotational flow. However, in most conditions, even though we make some supposes we can not obtain analytical solution. So we can not but tend to numerical simulation method. Actually, some structures with regular shape like cylinders maybe use special function such as Bessel function to get ideal analytical solution. According to reference 8, through comprehensively considering Navie-Stokes equations and continuity equation the FEM equations with displacement-pressure scheme (u_i, p) of uniform, inviscid and

compressible fluids under condition of small fluctuation are constructed.

2.1 The dynamics model of fluid-solid interaction system and its basic equations and boundary conditions

Here we suppose that water is inviscid, compressible and suffers small disturbance. At the same time, we can know that water's free surface appears small fluctuation because aqueduct locates in low seismic intensity area. We take aqueduct structures as linear elastic body because during the course of operation the aqueduct structures don't allow cracking. Here, V_s and V_f respectively represent solid domain and fluid domain. S_0 stands for interfaces between solid and fluid. S_b is fluid rigid fixed interfaces. S_f is defined as water's free surface. S_u is solid displacement boundaries. S_s stands for forces boundaries imposed on solid. \mathbf{n}_f is external normal line unit vector of fluid boundaries. \mathbf{n}_s is external normal line unit vector of solid boundaries. Any point at interfaces between solids and fluids \mathbf{n}_s and \mathbf{n}_f are opposite directions.

2.1.1 Fluid domain (V_f)

The equations for fluid field are listed as follows:

$$p_{,ii} - \frac{1}{c_0^2} \ddot{p} = 0 \quad (1)$$

Here p is fluid pressure and c_0 stands for sound velocity in fluids.

2.1.2 The boundary conditions of fluids

On rigid fixed boundary conditions (S_b):

$$\frac{\partial p}{\partial n_f} = 0 \quad (2)$$

On water's free surface (S_f):

$$\frac{\partial p}{\partial z} + \frac{1}{g} \ddot{p} = 0 \quad (3)$$

2.1.3 Solid domain (V_s)

The equations for solid field are expressed as follows:

$$s_{ij,j} + f_i = r_s \ddot{u}_i \quad (4)$$

Here s_{ij} are solid's stress components, u_i are solid's displacement components, f_i are solid's body force components, r_s stands for solid's density.

2.1.4 Solid body boundary conditions

The force boundary conditions (S_s) can be expressed as follows:

$$s_{ij} n_{sj} = \bar{T}_i \quad (5)$$

The displacement boundary conditions (S_u) can be written as follows:

$$u_i = \bar{u}_i \quad (6)$$

Here \bar{T}_i and \bar{u}_i respectively represent the known surface force components and displacement components.

2.1.5 Conditions on interfaces between solids and fluids

Kinetic conditions on the interfaces (S_0) are that normal velocity should keep continuous:

$$v_{fn} = \mathbf{v}_f \cdot \mathbf{n}_f = \mathbf{v}_s \cdot \mathbf{n}_f = -\mathbf{v}_s \cdot \mathbf{n}_s = v_{sn} \quad (7)$$

By means of motion equation of inviscid, weakly disturbed fluids, the equation 7 can be changed as follows:

$$\frac{\partial p}{\partial n_f} + \rho_f \mathbf{u} \cdot \mathbf{n}_f = 0 \quad (\text{on interfaces } S_0) \quad (8)$$

Here \mathbf{u} stand for solid's displacement vectors, ρ_f is fluid's density.

The continuous conditions of force on interfaces (S_0) are expressed as follows:

$$S_{ij}n_{sj} = t_{ij}n_{fj} = -t_{ij}n_{sj} \quad (9)$$

The equation 9 means that normal forces on interfaces are continuous. Here t_{ij} stand for fluid's stress tensor components. If the fluids are inviscid then t_{ij} can be written as follows:

$$t_{ij} = -pd_{ij} \quad (10)$$

By substitution equation 10 into equation 9 we can get:

$$S_{ij}n_{sj} = pn_{si} \quad (\text{on interfaces } S_0) \quad (11)$$

2.2 Establishment of fluid-solid interaction FEM equations based on Galerkin Method

2.2.1 Constructing interpolation function

For fluids pressure pattern is applied and pressure distribution in fluid's element can be expressed as follows:

$$p(x, y, z, t) \approx \sum_{i=1}^{m_f} N_i(x, y, z) p_i(t) = \mathbf{N}\mathbf{p}^e \quad (12)$$

Here m_f are node numbers of fluid elements, \mathbf{p}^e are node pressure vectors of fluid elements, N_i is interpolation function corresponding to node No. i , \mathbf{N} is interpolation function matrix.

For solid bodies displacement pattern is used and displacement distribution in solid element can be listed as follows:

$$\mathbf{u}(x, y, z, t) = \begin{pmatrix} u \\ v \\ w \end{pmatrix} \approx \sum_{i=1}^{m_s} \bar{N}_i(x, y, z) \begin{pmatrix} u_i \\ v_i \\ w_i \end{pmatrix} = \sum_{i=1}^{m_s} \bar{N}_i(x, y, z) \mathbf{a}_i(t) = \bar{\mathbf{N}}\mathbf{a}^e \quad (13)$$

Here m_s are node numbers of solid elements, \mathbf{a}^e are node displacement vectors of solid elements, \bar{N}_i is interpolation function corresponding to node No. i , $\bar{\mathbf{N}}$ is interpolation function matrix.

2.2.2 Derived solving equations by means of Galerkin Method

The weighted residual solution of Galerkin Method for basic equations and boundary conditions of fluid-solid interaction in fluid domain can be written as follows:

$$\int_{V_f} d p \left(p_{,ii} - \frac{1}{c_0^2} \rho \right) dV - \int_{S_b} d p \left(\frac{\partial p}{\partial n_f} \right) dS - \int_{S_f} d p \left(\frac{1}{g} \rho + \frac{\partial p}{\partial z} \right) dS - \int_{S_0} d p \left(\frac{\partial p}{\partial n_f} + \rho_f \mathbf{u} \cdot \mathbf{n}_f \right) dS = 0 \quad (14)$$

For solid domain supposed that displacement boundary conditions have been satisfied and then the formulas in solid domain can be expressed:

$$\int_{V_f} du_i (s_{ij,j} + f_i - r_s \sigma_{ij}) dV - \int_{S_s} du_i (s_{ij} n_{sj} - \bar{T}_i) dS - \int_{S_0} du_i (s_{ij} n_{sj} - p n_{si}) dS = 0 \quad (15)$$

Through application of integration by parts to first item $\int_{V_f} dp(p_{,ii}) dV$ of formula (14), we can obtain formula (16):

$$\int_{V_f} [(dp_{,i}) p_{,i} + \frac{1}{c_0^2} \sigma_{ij} \sigma_{ij}] dV + \int_{S_f} dp \left(\frac{1}{g} \sigma_{ij} n_{sj} \right) dS + \int_{S_0} dp (r_f \sigma_{ij} n_{sj}) dS = 0 \quad (16)$$

Similarly by use of integration by parts to first item $\int_{V_s} du_i (s_{ij,j}) dV$ of formula (15) and substituting it into physical equations, then we can get formula:

$$\int_{V_s} [de_{ij} D_{ijkl} e_{kl} - f_i + du_i (r_s \sigma_{ij})] dV - \int_{S_s} du_i \bar{T}_i dS + \int_{S_0} du_i (p n_{si}) dS = 0 \quad (17)$$

By substitution formula (12) and formula (13) into formula (16) and formula (17) respectively and at the same time considering the arbitrariness of dp and du_i , the FEM equations of fluid-solid interaction can be expressed as follows:

$$\begin{bmatrix} \mathbf{M}_s & 0 \\ -\mathbf{Q}^T & \mathbf{M}_f \end{bmatrix} \begin{pmatrix} \mathbf{a} \\ \mathbf{p} \end{pmatrix} + \begin{bmatrix} \mathbf{K}_s & \frac{1}{r_f} \mathbf{Q} \\ 0 & \mathbf{K}_f \end{bmatrix} \begin{pmatrix} \mathbf{a} \\ \mathbf{p} \end{pmatrix} = \begin{pmatrix} \mathbf{F}_s \\ 0 \end{pmatrix} \quad (18)$$

Here \mathbf{p} are pressure vectors on fluid's nodes, \mathbf{a} are displacement vectors on solid's nodes, \mathbf{Q} is fluid-solid coupling matrix, \mathbf{M}_f and \mathbf{K}_f are global fluid mass matrix and global fluid stiffness matrix respectively, \mathbf{M}_s and \mathbf{K}_s are global solid mass matrix and global solid stiffness matrix respectively, \mathbf{F}_s are external loads vectors imposed on solids. Each element matrix corresponding to global matrixes can be expressed:

$$\mathbf{M}_f^e = \int_{V_f^e} \frac{1}{c_0^2} \mathbf{N}^T \mathbf{N} dV + \int_{S_f^e} \frac{1}{g} \mathbf{N}^T \mathbf{N} dS ; \quad \mathbf{K}_f^e = \int_{V_f^e} \frac{\partial \mathbf{N}^T}{\partial x_i} \frac{\partial \mathbf{N}}{\partial x_i} dV ; \quad \mathbf{Q}^e = \int_{S_0^e} r_f \bar{\mathbf{N}}^T \mathbf{n}_s \mathbf{N} dS ; \quad \mathbf{M}_s^e = \int_{V_s^e} r_s \bar{\mathbf{N}}^T \mathbf{N} dV ;$$

$$\mathbf{K}_s^e = \int_{V_s^e} \mathbf{B}^T \mathbf{D} \mathbf{B} dV ; \quad \mathbf{F}_s^e = \int_{V_s^e} \mathbf{N}^T \mathbf{f} dV + \int_{S_s^e} \mathbf{N}^T \bar{\mathbf{T}} dS \quad , \text{ here } \mathbf{B} \text{ is displacement-strain relation matrix of solids. From}$$

above calculation process we can see that \mathbf{M}_f^e consists of two parts. The first part is \mathbf{M}_{fV}^e and the second part is \mathbf{M}_{fs}^e . So we can know that $\mathbf{M}_f^e = \mathbf{M}_{fV}^e + \mathbf{M}_{fs}^e$. Here \mathbf{M}_{fV}^e is element mass matrix caused by compressible fluids, \mathbf{M}_{fs}^e is element mass matrix caused by free surface wave problems. When considering the response of aqueduct under condition of earthquake, the FEM equations of fluid-solid interaction can be written as follows:

$$\begin{bmatrix} \mathbf{M}_s & 0 \\ -\mathbf{Q}^T & \mathbf{M}_f \end{bmatrix} \begin{pmatrix} \mathbf{a} \\ \mathbf{p} \end{pmatrix} + a \begin{bmatrix} \mathbf{M}_s & 0 \\ -\mathbf{Q}^T & \mathbf{M}_f \end{bmatrix} \begin{pmatrix} \mathbf{a} \\ \mathbf{p} \end{pmatrix} + b \begin{bmatrix} \mathbf{K}_s & \frac{1}{r_f} \mathbf{Q} \\ 0 & \mathbf{K}_f \end{bmatrix} \begin{pmatrix} \mathbf{a} \\ \mathbf{p} \end{pmatrix} + \begin{bmatrix} \mathbf{K}_s & \frac{1}{r_f} \mathbf{Q} \\ 0 & \mathbf{K}_f \end{bmatrix} \begin{pmatrix} \mathbf{a} \\ \mathbf{p} \end{pmatrix} = \begin{pmatrix} \mathbf{F}_s \\ 0 \end{pmatrix} \quad (19)$$

Here $C = a \begin{bmatrix} M_s & 0 \\ -Q^T & M_f \end{bmatrix} \begin{pmatrix} \dot{x} \\ \dot{p} \end{pmatrix} + b \begin{bmatrix} K_s & \frac{1}{r_f} Q \\ 0 & K_f \end{bmatrix} \begin{pmatrix} x \\ p \end{pmatrix}$ is damping matrix, a and b are proportional mass and stiffness damping coefficients respectively.

3.FEM MODEL OF AQUEDUCT

Caohe Aqueduct locates in Shenxing Town, Mancheng County, Baoding City, Hebei Province. This aqueduct is a large span cross structures in South-to-North Water Diversion Middle Line Project. The designed discharge is $125 m^3/s$, the maximum designed discharge is $150 m^3/s$. The span of aqueduct is 30m and the structure of single connection of three flumes with multi-side walls is applied. Each flume's cross section size is $6.0 \times 5.4m$ and the thickness of side wall is 0.6m. At the top of side walls 2m thick pedestrian plates are paved. The thickness of middle walls between each flume is 0.7m. Similarly, 2.7m thick pedestrian plates are paved on the top of middle walls. Longitudinal prestressed structures are used by side walls and middle walls. Side ribs and bottom ribs are fixed in aqueduct body. On the top of the side walls and middle walls, pull rods are also constructed. The spacing of side ribs is 2.5m, the wideness and height of side ribs are 0.5m and 0.7m respectively. The spacing of bottom ribs is also 2.5m, the wideness and height of bottom ribs are 0.5m and 1.1m respectively. The wideness and height of pull rods are 0.3m and 0.4m respectively. The material of aqueduct is C50 grade reinforced concrete which maximum compressive strength is about 50MPa.

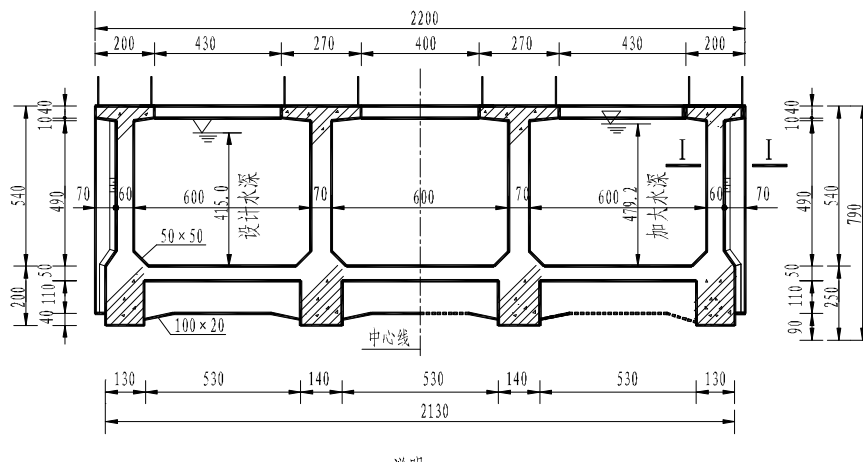


Figure one The cross section of aqueduct

3.1 The 3-D FEM model

The single-span aqueduct is 30m long and 22m wide. In this paper tetrahedron element is used to calculate aqueduct structures. The rod element is applied to simulate steel strand and some steel bars. A total number of 64115 elements are subdivided. The X-coordinate is in the same direction with water flow. The Y-coordinate is parallel to aqueduct's wide direction. The Z-coordinate is in the same direction with elevation of aqueduct. The 3-D FEM model is obtained by soft ANSYS.

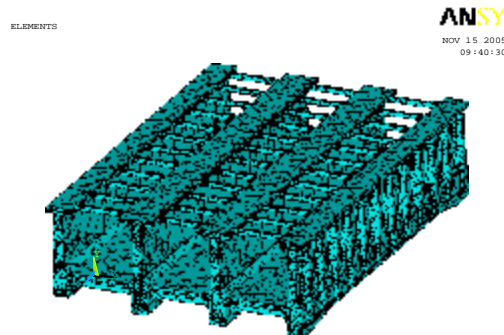


Figure two The 3-D FEM model of aqueduct

3.2 Calculation cases

In order to ensure safe operation and obtain reliable economic benefit, it is necessary to take numerical simulation on high strength and large span aqueduct structures. According to engineering practice and project construction planning, six calculation cases are chosen in this paper. ①three flumes passing water under condition of designed water depth(4.15m) and considering aqueduct gravity; ②three flumes passing water under condition of increased water depth(4.792m) and considering aqueduct gravity; ③three flumes passing water under condition of bankfull water depth(5.4m) and considering aqueduct gravity; ④three flumes passing water under condition of bankfull water depth(5.4m) and considering aqueduct gravity and wind load; ⑤only middle flume passing water under condition of increased water depth(4.792m) and considering aqueduct gravity; ⑥only two side flumes passing water under condition of increased water depth(4.792m) and considering aqueduct gravity. The calculation software was self-developed and this software could interface with ANSYS and Autocad. In the past five years, the software have been successfully applied to some huge hydropower project in China, such as Three Gorges Project, Jinping arch dam and Xiaowan arch dam.

3.3 The choosing of seismic waves

When taking seismic response calculation on aqueduct, it is necessary to choose reasonable seismic waves because waveforms have profound effect on seismic response of aqueduct. According to site conditions of aqueduct, for the sake of thoroughly reflecting seismic response of aqueduct under condition of different seismic waves, in this paper EL-Centro wave, Taft wave, Pasadena wave are chosen as ground acceleration. The seismic waves input methods listed as follows: when transverse excitation source happening then EW component of EL-Centro wave, Taft wave, Pasadena wave should be inputted. If vertical excitation source taking place, then NS component of EL-Centro wave, Taft wave have to be inputted. The concrete numerical values and maximum amplitude are confirmed according to reference [15].

3.4 Calculation results

Before undertaking dynamic analysis water can be taken as a kind of additional mass of aqueduct structure. When calculation we can know that in the intake and outlet of aqueduct water is free and the boundary conditions in intake and outlet of aqueduct are $\partial p / \partial n = 0$. Calculation results mainly include three parts. The first part is transverse displacement in bottom plates in the middle of three flumes respectively. The second part is longitudinal displacement in bottom plates in the middle of three flumes respectively. The three part is rotation angle of middle cross section intertwining axis of three flumes respectively (because of more calculation cases, the calculated stresses and displacement contour plots are cancelled). Main calculation results are listed as follows:

3.4.1 Transverse displacement in bottom plates in the middle of three flumes

The maximum transverse displacement in bottom plates in the middle of three flumes respectively are listed in table one under condition of EW component excitation of EL-Centro wave, Taft wave, Pasadena wave. From table one we can know that the distribution law and changing trend of transverse displacement in bottom plates in the middle of three flumes are similar. However, transverse displacement in bottom plates in the middle flume is bigger than that of in two side flumes. With water depth increasing, the mass of aqueduct increases too. As a result, transverse displacement in bottom plates in the middle of three flumes is gradually increased. Furthermore, under condition of cross-wind loads action, transverse displacement in bottom plates in the middle of three flumes is a little larger than that of without considering cross-wing load action. The increasing amplitude is not obvious which indicates that water can effectively reduce transverse seismic response.

Figure 1 the maximum transverse displacement in bottom plates
 in the middle of three flumes

position	Maximum transverse displacement (mm)					
	case①	case②	case③	case④	case⑤	case⑥
Bottom plate in the middle of right flume	66.382	70.793	75.811	77.972	68.652	69.389
Bottom plate in middle flume	72.831	76.443	83.935	86.384	74.915	74.227
Bottom plate in the middle of left flume	67.153	69.002	75.334	77.932	68.306	70.021

3.4.2 Rotation angle of middle cross section intertwining axis of three flumes

The maximum rotation angle of middle cross section intertwining axis of three flumes respectively are listed in table two under condition of EW component excitation of EL-Centro wave, Taft wave, Pasadena wave. From calculation results, the distribution law and changing trend of rotation angle of middle cross section intertwining axis of three flumes are same. Actually, rotation angle in the middle flume is bigger than that of two side flumes. Similarly, considering cross-wind loads action the maximum rotation angle of middle cross section intertwining axis of three flumes respectively are larger that that of without considering cross-wind loads. With water depth increasing, the mass of aqueduct increases too. As a result, the maximum rotation angle of middle cross section intertwining axis of three flumes respectively increases too. In fact, the distribution law and changing trend of rotation angle of middle cross section intertwining axis of three flumes before and after water level changing are same. So we can know that fluid-solid interaction obviously affects the value of rotation angle but less obviously affects distribution law of rotation angle. Fluid-solid interaction calculation also indicates that seismic response aroused by longitudinal waves is less than that of transverse waves.

Table 2 The maximum rotation angle of middle cross section intertwining axis of three flumes

position	Maximum rotation angle (rad)					
	case①	case②	case③	case④	case⑤	case⑥
Cross section in the middle of right flume	0.115	0.131	0.152	0.153	0.127	0.128
Cross section in middle flume	0.119	0.137	0.158	0.161	0.131	0.130
Cross section in the middle of left flume	0.113	0.133	0.153	0.155	0.126	0.129

3.4.3 Longitudinal displacement in bottom plates in the middle of three flumes

The maximum longitudinal displacement in bottom plates in the middle of three flumes respectively are listed in table three under condition of NS component excitation of EL-Centro wave, Taft wave. From calculation results we can know that the maximum longitudinal displacement takes place in farthest point on aqueduct along seismic transmission direction (right flume is far from that of seismic source). However, no matter whether considering fluid-solid interaction or not, with water depth increasing, the mass of aqueduct increases too. As a result, longitudinal displacement in bottom plates in the middle of three flumes is gradually increased. Furthermore, under condition of cross-wind loads action, longitudinal displacement in bottom plates in the middle of three flumes is a little larger than that of without considering cross-wing load action. The increasing amplitude is not obvious which indicates that water can effectively reduce longitudinal seismic response. Transverse waves impose little effect on longitudinal displacement.

Table 3 the maximum longitudinal displacement in bottom plates in the middle of three flumes

position	Maximum longitudinal displacement (mm)					
	case①	case②	case③	case④	case⑤	case⑥
Bottom plate in the middle of right flume	1.92	2.11	2.33	2.85	2.04	2.05
Bottom plate in middle flume	1.55	1.71	1.88	1.92	1.69	1.69
Bottom plate in the middle of left flume	1.88	2.09	2.30	2.73	1.99	2.03

3.4.4 Vertical displacement in bottom plates in the middle of three flumes

The maximum vertical displacement in bottom plates in the middle of three flumes aroused by transverse waves and longitudinal waves are very small respectively. Calculation indicates that no matter whether considering fluid-solid interaction or not the vertical displacement changes a little. It shows that fluid-solid interaction has little influence on aqueduct vertical displacement.

4. CONCLUSIONS

- (1) Results of different calculation cases indicate that considering fluid-solid interaction in aqueduct and different water depth have close relation with aqueduct seismic response. It is necessary to study fluid-solid interaction mechanism under condition of seismic waves action[15].
- (2) Different seismic response can be obtain under condition of different seismic waves excitation. Although calculation results changing trends are similar the values of results are different. So, in practical project we must

consider reasonable excitation direction and seismic waves.

(3) Under condition of cross-wind loads action the maximum longitudinal and transverse displacements are a little larger than that of without cross-wind action. It indicates that water body can effectively reduce seismic response of aqueduct.

(4) The maximum longitudinal displacement aroused by transverse waves is very small. The seismic response of aqueduct brought by longitudinal waves action is less than that of transverse waves action.

ACKNOWLEDGEMENT: This research was supported by National Natural Science Foundation of China (NSFC, with granted number: 50679036). We thank Professor Huang Da-hai for comments on the manuscript.

REFERENCES

- [1] Westergaard H M. Water pressures on dams during earthquakes[J]. *Trans. of American Society of Civil Engineering*, 1933, 59 (3) :418 - 472.
- [2] Zheng Zhe-min. The vibration of plates under condition of fluids action[J]. *Acta Mechanica Sinica*, 1958, 2 (1) : 11-16.
- [3] Zheng Zhe-min, Ma Zong-kui. Free vibration of cantilever under condition of lateral fluids action[J]. *Acta Mechanica Sinica*, 1959, 3 (2) :111 - 120.
- [4] Gpeanspan J E. Fluid-solid interaction[A]. *The Winter Annual Meeting of the ASME*[C]. Pittsbergh, Pennsylvania, 1967.
- [5] Bishop R E D , Price W G. *Hydroelasticity of Ships*[M]. Cambridge :Cambridge University Press, 1979.
- [6] Zienkiewicz O C, Bettess P. Fluid-structure dynamic interaction and wave forces: An Introduction to numerical treatment [J] . *International Journal for Numerical Methods in Engineering* , 1978 ,13 (1) :1 - 16.
- [7] FENG Zhenxing , Hung T C. The coupled BE/ FE algorithm for fluid2structure interaction : 2-D and 3-D numerical results[J] . *Acta Mechanica and Scientia* , 1987 ,7(2) .
- [8] Lu Xin-sen. *Advanced Structural Dynamics*[M]. Shanghai: Shanghai Jiaotong University Press, 1992.
- [9] Alfredo B, Rodolfo R. Finite element computation of the vibration modes of a fluid-solid system, [J]. *Comput Methods, Appl Mesh Eugrg*, 1994, 119-120.
- [10] Alfredo B, Rodolfo R, Rodriguez R. Finite element solution of incomp resible fluid-structure vibration p roblems [J]. *International Journal for numericalmethod in engineering*, 1997:40-42.
- [11] Liu W K, Chang H G. Multidisciplinary and interaction problems: A method of computation for fluid structure interaction,[J] *Computer & Structure*, 1985, 20 :1-3.
- [12] Dai Da-nong, Wang Xu-cheng, Du Qing-hua. A model analysis for the dynamic response of fluid-structure systems[J]. *Acta Mechnica Solida Sinica*, 1990, 11 (4) : 305 - 312
- [13] Jin Zhan-li, Wang Zong-li, Li Hong-yun. Numerical Computing Method of Additional Water Mass when the Structure Vibrates in the Infinite Liquid[J]. *Journal of Shanghai Jiaotong University*, 2000, 34 (8).
- [14] Wang Xu-cheng. *Finite Element Method*[M]. Beijing: Tsinghua University Press, July, 2003.
- [15] Wang Bo, Chen Huai, Xu Wei. Nonlinear seismic response analysis of aqueduct constructed with lead rubber bearing for vibration isolation [J]. *Water Resources and Hydropower Engineering*, June, 2005, Vol.25 No.3:5-7.